

Pressure-induced phonon frequency shifts in transition-metal nitridesXiao-Jia Chen, Viktor V. Struzhkin, Simon Kung,* Ho-kwang Mao, and Russell J. Hemley
*Geophysical Laboratory, Carnegie Institution of Washington, Washington, DC 20015, USA*Axel Nørnlund Christensen
Højksøvej 7, DK-8210 Aarhus V, Denmark

(Received 9 January 2004; revised manuscript received 15 March 2004; published 1 July 2004)

We report the experiments on the high-pressure phonon spectra of transition-metal nitrides HfN, ZrN, and NbN, obtained by Raman-scattering measurements. Two pronounced bands, which are related to the acoustic part at low-frequency around 200 cm^{-1} and the optical part at high-frequency around 550 cm^{-1} of the phonon spectrum, respectively, shift to high-frequency values with increasing pressure. An analysis of the results allows us to reproduce the experimental pressure dependence of the superconducting transition temperature T_c of ZrN and NbN. We also predict the pressure effect on T_c in HfN.

DOI: 10.1103/PhysRevB.70.014501

PACS number(s): 74.62.Fj, 78.30.Er, 74.70.Ad

I. INTRODUCTION

When pressure is applied to a superconducting material the superconducting transition temperature T_c generally changes. In contrast to the decrease of T_c generally observed when a nontransition-metal superconductor is subjected to high-pressure, many of the transition metals and their alloys and compounds exhibit an increase in T_c .¹ The recent development of new high-pressure techniques for electric and magnetic measurements in a diamond-anvil cell (DAC) makes possible the investigation of the pressure dependence of T_c at megabar range.^{2,3} A significant increase in T_c with pressure up to 120 GPa has been observed in some transition metals,^{4,5} pointing to the possibility of obtaining high T_c 's at high-pressures in their alloys and compounds. Compared to the elements, transition metal carbide, and nitride compounds have relatively high values of T_c at ambient condition, reaching nearly 18 K in $\text{NbC}_{0.3}\text{N}_{0.7}$.⁶ Earlier studies⁷⁻¹⁰ have revealed that application of pressure increases T_c in NbN,⁷ VN,⁸ and TaN,⁹ while in NbC,¹⁰ ZrN,¹⁰ and TaC⁹ the value of T_c decreases. Therefore, it is of considerable physical interest to investigate superconductivity at very high-pressures in these compounds.

It is well established¹¹ that the relatively high T_c 's in transition metal carbides and nitrides are attributed to a softness of the lattice against hydrostatic deformations, which gives rise to strong electron longitudinal-acoustic coupling. Neutron scattering measurements^{12,13} have shown that some superconducting carbides always have anomalies in their phonon dispersion curves, whereas nonsuperconducting carbides do not exhibit anomalies. Anomalies in the dispersion of the acoustic branches similar to those reported for the superconducting carbides have also been detected in superconducting transition-metal nitrides¹⁴⁻¹⁷ by inelastic neutron-scattering as well. These data also provide important insight into the relationship between superconductivity and lattice instabilities. However, currently the information concerning the change in the characteristic phonon spectra under pressure in these compounds is nonexistent, due to the difficulties of neutron-scattering experiments, particularly under pressure.

The present investigation was undertaken for purposes of obtaining data on the changes in lattice vibrations under pressure in selected transition-metal nitrides, and to ascertain the contribution of the electron-phonon interaction to different characteristics of the pressure effects on T_c in these materials. We performed the high-pressure Raman-scattering measurements on single crystals of HfN, ZrN, and NbN. High-pressure phonon spectra up to 30 GPa were obtained. The phonon densities obtained from neutron-scattering are compared with Raman spectra. We show that the pressure-induced phonon frequency shifts are essential for understanding the pressure effects on T_c in these compounds.

II. EXPERIMENTAL TECHNIQUES

Single crystals of HfN, ZrN, and NbN were grown by the zone-annealing technique which has been detailed previously.¹⁵⁻¹⁷ Rods of hafnium, zirconium, and niobium with higher than 99.9% purity were zone annealed in a nitrogen atmosphere of nominal 99.99% purity under a pressure of 2 MPa at a temperature regime from 2100 to 3000°C. Specimens for Raman-scattering measurements and structural study were cut from the crystal. Synchrotron x-ray diffraction data collected at Argonne National Laboratory will be described elsewhere.¹⁸

Our high-pressure Raman system has been described previously.^{19,20} For nontransparent and highly reflective samples, a "quasibackscattering" (or angular) geometry is employed. This arrangement has the advantage that the specular reflection (or direct laser beam in the case of forward scattering) is directed away from the spectrometer. Compared with the backscattering geometry, this expedient reduces the overall background, and allows the observation of lower-frequency excitations. In the case of metals, use of the angular excitation geometry was found to be crucial.¹⁹ To be compatible with this geometry the diamond seat is modified to allow off-axis entry of the incident light. Specially designed tungsten carbide seats having angular conical holes were used for this purpose. We have used synthetic ultrapure anvils to reduce diamond fluorescence. Samples were loaded

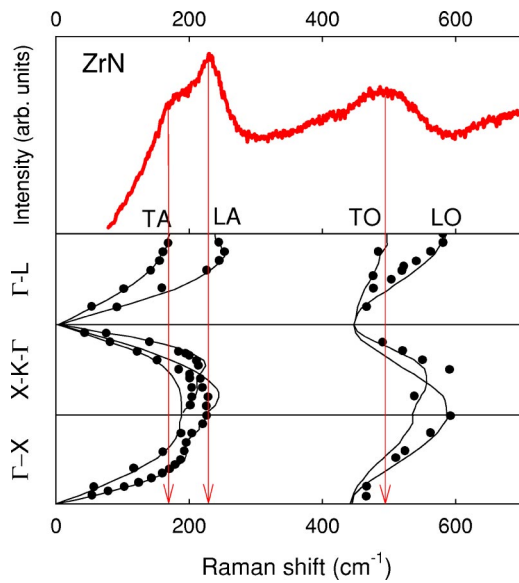


FIG. 1. (Color online) Ambient pressure Raman spectra of ZrN (top panel) and neutron inelastic scattering results taken from Ref. 15 (lower panels) for the phonon dispersion in ZrN.

into the DAC without any pressure medium and pressure was determined using ruby fluorescence technique. Argon ion laser operating at 514 or 488 nm was used for excitation of Raman signals, the laser power on the sample in DAC was about 100 mWt. A typical Raman spectrum from ZrN is compared to the neutron-inelastic-scattering results¹⁵ in Fig. 1. The detailed discussion of the comparison between the Raman and neutron-scatterings for ZrN as well as other nitrides will be given in the next section.

III. PRESSURE EFFECT ON PHONON SPECTRA

Extensive studies^{21–23} have proven Raman scattering to be a powerful tool in revealing phonon anomalies in transition-metal nitrides, because of the good agreement between the phonon densities obtained from neutron scattering and the Raman spectra similar to the one-phonon density of states. The Stokes sides of the Raman spectrum up to 800 cm^{-1} as a

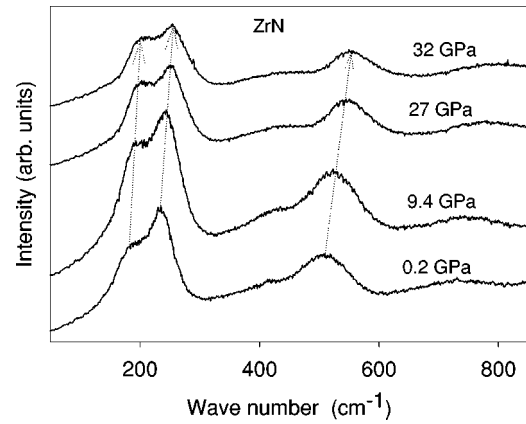


FIG. 3. Raman scattering intensity of a ZrN single crystal measured under various pressures.

function of pressure for HfN, ZrN, and NbN are shown in Figs. 2–4. The spectrum exhibits two pronounced bands, which are related to the acoustic part and the optical part of the phonon spectrum, respectively. The pressure dependence of the Raman peaks in the low-frequency and high-frequency range is summarized in Table I.

As can be seen from Fig. 2, transverse and longitudinal branches for Hf vibrations at the BZ boundary ($\sim 200 \text{ cm}^{-1}$) are well resolved, as well as the higher frequency nitrogen band ($\sim 500\text{--}600 \text{ cm}^{-1}$). The low-frequency scattering is caused by acoustic phonons, and the high-frequency scattering is due to optical phonons. With increasing pressure, the two scattering bands shift to higher frequencies. The two peaks in the acoustic range as well as the high-frequency optical branch are in close agreement with the phonon density of states obtained from neutron-scattering data in HfN.¹⁶

Similar to HfN, transverse and longitudinal acoustic bands for Zr shown in Fig. 3 are well resolved, however, they are located at higher frequencies since Zr atoms are lighter than Hf atoms. An additional weak band around 700 cm^{-1} may belong to second-order scattering. At ambient condition, the spectrum of ZrN is dominated by strong peaks at 178, 230, and 497 cm^{-1} . These characteristics are very

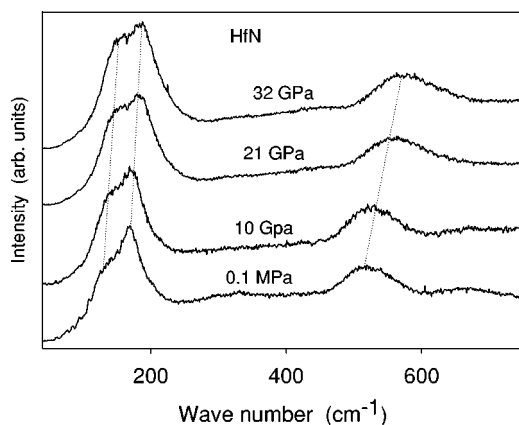


FIG. 2. Raman scattering intensity of a HfN single crystal measured under various pressures.

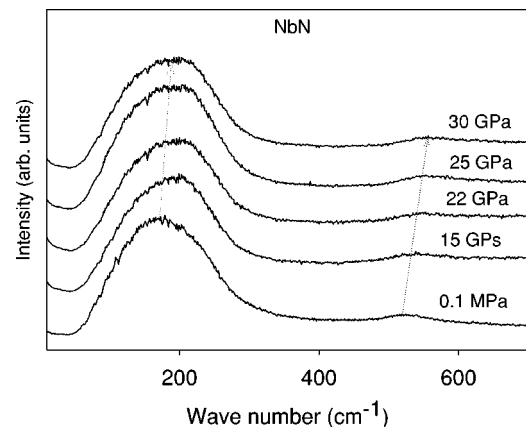


FIG. 4. Raman scattering intensity of a NbN single crystal measured under various pressures.

TABLE I. Pressure dependence of the low-frequency (LF) and high-frequency (HF) Raman peaks of the superconducting transition-metal nitrides HfN, ZrN, and NbN.

HfN			ZrN				NbN			
P (GPa)	ω_{LF1} (cm^{-1})	ω_{LF2} (cm^{-1})	ω_{HF} (cm^{-1})	P (GPa)	ω_{LF1} (cm^{-1})	ω_{LF2} (cm^{-1})	ω_{HF} (cm^{-1})	P (GPa)	ω_{HF} (cm^{-1})	ω_{HF} (cm^{-1})
0	125	169	521	0.2	179	232	506	0	182	523
10	136	171	528	9.4	189	243	521	15	190	558
21	146	179	564	27	196	250	547	22	189	571
32	149	187	576	32	201	255	552	25	189	575
								30	186	572

similar to the previous Raman measurements.²² The frequency range of high-phonon density of states determined from the coherent-inelastic-neutron scattering²⁴ is from 150 to 260 cm^{-1} for the low-frequency acoustic branch and around 500 cm^{-1} for the optical branch, respectively. The application of pressure shifts the peak frequency to higher values. This behavior is similar to the case in HfN shown in Fig. 2. Since the good agreement (see Fig. 1) between the Raman spectra and the phonon densities,²⁴ this shift indicates pressure-induced phonon hardening.

Measured high-pressure Raman spectra of NbN are shown in Fig. 4. The high-frequency optical branch shows the same overall behavior as HfN and ZrN. Here, transverse and longitudinal Nb bands around 190 cm^{-1} are not well resolved. The relative intensity of the high-frequency (600 cm^{-1}) nitrogen band is much lower than in the homologous HfN and ZrN samples. In comparison with the two peaks of the acoustic part observed in HfN and ZrN, the low-frequency acoustic part of NbN has two interesting features. First, there is only a broad-frequency peak around 190 cm^{-1} in NbN. The relatively broad line shape indicates anomalies in the phonon spectra of NbN. Another prominent feature is the insensitivity of the broad peak to pressure.

Information regarding the Raman frequency shift with pressure in these materials should help elucidate the pressure effect on T_c . Suppose the two atoms in the unit cell are labeled T and N for transition metal and nitrogen and their masses are represented by M_T and M_N , respectively ($M_T \gg M_N$). The product of the mean-square frequencies $\langle \omega^2 \rangle$ and the mass M was obtained from the Raman spectra in terms of the relation²⁵ $M\langle \omega^2 \rangle = M_s\langle \omega_{ac}^2 \rangle + M_r\langle \omega_{op}^2 \rangle$, where $M_s = M_T + M_N$ and $M_r^{-1} = M_T^{-1} + M_N^{-1}$. Because of the large mass ratio between the transition-metal and the nitrogen atoms, the mass M_s is nearly equal to that of the metal atom and the reduced mass M_r is almost equal to those in nitrogen atoms. In transition-metal nitrides one has¹¹ $M_T\langle \omega_{ac}^2 \rangle = M_N\langle \omega_{op}^2 \rangle$, as one would expect from nearest-neighbor forces. Therefore, we have $\langle \omega^2 \rangle^{1/2} \approx (2M_T/M)^{1/2}\langle \omega_{ac}^2 \rangle^{1/2} \approx (2M_N/M)^{1/2}\langle \omega_{op}^2 \rangle^{1/2}$ for these materials. This implies that $d \ln \langle \omega^2 \rangle^{1/2} / dP = d \ln \langle \omega_{ac}^2 \rangle^{1/2} / dP = d \ln \langle \omega_{op}^2 \rangle^{1/2} / dP$. It is clear that the pressure-induced phonon frequency shift can be well represented by either the pressure-induced frequency shift of the acoustic branch or the shift of the optical frequency branch.

A tunneling experiment by Zeller²⁶ showed that the main contribution to the electron-phonon coupling constant λ

comes from the acoustic vibrations that correspond to predominantly metal atom vibrations. Furthermore, Spengler *et al.*²³ reported a close relationship between the first peak of the acoustic branch and the value of T_c in stoichiometric superconducting TiN. Whether or not the frequency of the acoustic part plays an important role in the pressure effect on T_c through the change of λ , it is interesting to see the pressure-induced change of the first peak in the acoustic range. The results from high-pressure Raman scattering are shown in Fig. 5. With the application of pressure, the peak frequency initially shifts to higher frequency in all of the nitrides studied. With further pressure increase, the frequency begins to decrease after reaching a maximum at around 15 GPa in NbN. However, pressure always increases the frequency peak in HfN and ZrN in the pressure range up to 32 GPa. Considering that $\lambda \propto \langle \omega_{ac}^2 \rangle^{-1}$ is valid approximately, these observations indicate that T_c would decrease with increasing pressure. Obviously, this behavior is not always true for transition metal nitrides. Thus, we expect that the interplay of the counteracting changes in $\langle \omega_{ac}^2 \rangle$ and the “electronic” part of λ due to pressure is responsible for the pressure dependence of T_c .

IV. PRESSURE EFFECTS ON T_c

For the analysis of the results on the superconducting transition temperature we start with McMillan’s T_c formula²⁷

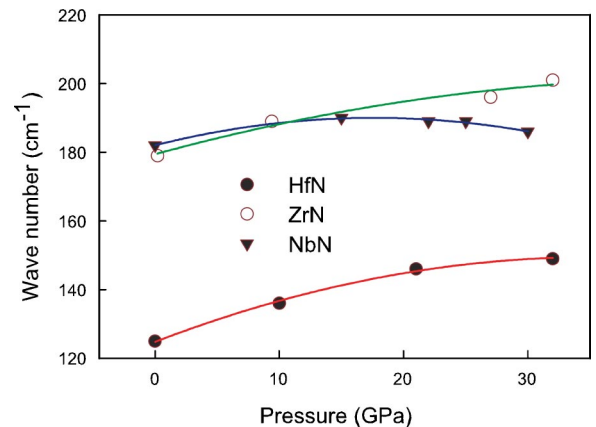


FIG. 5. (Color online) The pressure dependence of the frequency of the first peak of the acoustic branch in HfZ, ZrN, and NbN. The lines are guides to the eye.

$$T_c = \frac{\Theta_D}{1.45} \exp \left[- \frac{1.04(1+\lambda)}{\lambda - \mu^*(1+0.62\lambda)} \right], \quad (1)$$

which relates T_c to the electron-phonon coupling parameter λ , the Coulomb repulsion strength μ^* , and a temperature Θ_D characteristic of the phonons. Considering the variations of Θ_D , λ , and μ^* with pressure or volume and introducing parameters $\varphi = \partial \ln \lambda / \partial \ln V$ and $\xi = \partial \ln \mu^* / \partial \ln V$, we can get the pressure coefficient of T_c

$$\begin{aligned} \frac{d \ln T_c}{dP} &= \frac{\gamma_G}{B_0} - \frac{1.04\lambda(1+0.38\mu^*)}{[\lambda - \mu^*(1+0.62\lambda)]^2 B_0} \varphi \\ &+ \frac{1.04\mu^*(1+\lambda)(1+0.62\lambda)}{[\lambda - \mu^*(1+0.62\lambda)]^2 B_0} \xi, \end{aligned} \quad (2)$$

where $B_0 \equiv 1/\kappa_V = -\partial P / \partial \ln V$ is the bulk modulus and Θ_D is assumed to be proportional to $\langle \omega^2 \rangle^{1/2}$ and $\gamma_G = -\partial \ln \langle \omega^2 \rangle^{1/2} / \partial \ln V$ being the effective Grüneisen parameter.

The formula for μ^* due to Morel and Anderson²⁸ used here is

$$\mu^* = \frac{\mu}{1 + \mu \ln(E_F/\omega_{ph})}, \quad (3)$$

with $\mu = 0.5 \ln[(1+a^2)/a^2]$ and $a^2 = \pi e^2 N(E_F)/k_F^2$, where $N(E_F)$ is the electronic density of states at the Fermi energy E_F , from which we evaluate the volume dependence of μ^* as

$$\xi = \mu^* \left[\frac{2}{3} - \gamma_G - \frac{1 - e^{-2\mu}}{2\mu^2} \left(\gamma_N + \frac{2}{3} \right) \right]. \quad (4)$$

Here $\gamma_N = \partial \ln N(E_F) / \partial \ln V$ and the variation of k_F with volume has been calculated from the fundamental definition $k_F = (3\pi^2 Z/V)^{1/3}$ with Z the valency.

The electron-phonon coupling parameter λ can be expressed as

$$\lambda = \frac{N(E_F)\langle I^2 \rangle}{M\langle \omega^2 \rangle} \equiv \frac{\eta}{M\langle \omega^2 \rangle}, \quad (5)$$

where $\langle I^2 \rangle$ is the mean-square electron-ion matrix element and M the ionic mass. The McMillan-Hopfield parameter η is the electronic part of λ , which has a local ‘‘chemical’’ property of an atom in a crystal. Taking the logarithmic volume of Eq. (5), we find

$$\varphi = 2\gamma_G + \frac{\partial \ln \eta}{\partial \ln V}. \quad (6)$$

It has been found^{29,30} that the coefficient $\partial \ln \eta / \partial \ln V$ is close to

$$\frac{\partial \ln \eta}{\partial \ln V} = -\gamma_N - \frac{2}{3}. \quad (7)$$

Knowing B_0 , γ_G , and γ_N , one can calculate the pressure derivative of T_c using Eqs. (2), (4), (6), and (7).

We now show how the Raman results provide valuable information on the pressure effect on T_c . The structural parameter B_0 is taken to be 270 and 350 GPa for ZrN and NbN from the theoretical studies.³¹ Recent theoretical calculations

gave a value of B_0 of 344 K for HfN.¹⁸ Such values are consistent with early neutron scattering data.^{15–17} As seen in Fig. 5, the lowest frequency of the acoustic phonons initially increases with pressure. If we take the simplifying assumption that the measured lowest frequency peak ω_{LF1} can be used to replace $\langle \omega^2 \rangle^{1/2}$ over the whole frequency range, then we would have the initial value of $d \ln \langle \omega^2 \rangle^{1/2} / dP$ of 8.80×10^{-3} , 6.07×10^{-3} , and 2.93×10^{-3} GPa⁻¹ for HfN, ZrN, and NbN, respectively. Thus we have the corresponding lattice Grüneisen parameter $\gamma_G = 3.03, 1.64$, and 1.02 for the compounds studied. Band structure calculations^{32,33} show that the electronic density of states $N(E_F)$ initially decreases with pressure at a rate of $d \ln N(E_F) / dP = -3.60 \times 10^{-3}$ and -4.49×10^{-3} GPa⁻¹ for ZrN and NbN, respectively. Combining this calculated value and B_0 , we get $\gamma_N = 0.97$ for ZrN and 1.57 for NbN. At present, there is not a theoretical value of $d \ln N(E_F) / dP$ available for HfN. Considering that the effect of band shifting under pressure is to change significantly the density of states of the d electrons, we can estimate γ_N from the relation³⁴ $\gamma_N \approx \gamma_N^{(d)} \equiv q_0/l/3$. Here, l is nearest-neighbor interatomic distance and q_0 is obtained from the tables of Hartree-Fock atomic wave functions of the d electrons with $\Psi_d \propto e^{-q_0 l}$. For HfN, Hanfe *et al.*³⁵ gave a $q_0 l$ of 3.7. We then have $\gamma_N = 1.23$. Using Eqs. (6) and (7), we obtain the value of φ of 4.15, 1.64, and -0.24 for HfN, ZrN, and NbN, respectively. The volume dependence of μ^* can be derived from Eq. (4) once having the values of γ_G , γ_N , μ^* , and μ . Since a^2 has a typical value of 0.4,²⁸ we have $\mu = 0.63$. Studies of the isotopic mass dependence of T_c and the inversion of superconducting tunneling curves have revealed that μ^* values all lay in the range between 0.1 and 0.2. The Coulomb pseudopotential μ^* was determined to be 0.11, 0.11, 0.13 for HfN, ZrN, and NbN, respectively.³⁴ Based on these parameters, we obtain the corresponding ξ of -0.45 , -0.27 , and -0.30 for these compounds. We summarized these parameters used in Table II.

The heat capacity measurements yield the Debye temperature Θ_D of 412, 515, and 363 K for HfN, ZrN, and NbN, respectively.³⁶ Substituting the experimentally determined T_c 's of 8.83, 10.00, and 14.94 K gives the corresponding electron-phonon coupling constant λ of 0.643, 0.627, and 0.906. With the parameters determined listed in Table II, we have calculated the pressure derivative of T_c by using Eq. (2). The calculated dT_c/dP is -0.24 , -0.13 , and 0.05 K/GPa for HfN, ZrN, and NbN, respectively. The sign of our calculated dT_c/dP for ZrN and NbN clearly agrees with the experimental data.^{7,10} Therefore, Raman scattering under high pressure indeed provides essential information for understanding of the pressure effect on T_c . The calculated dT_c/dP of 0.05 K/GPa for NbN is in excellent agreement with the measured value of 0.04 K/GPa.⁷ For ZrN, Smith¹⁰ reported a dT_c/dP of -0.17 K/GPa from high-pressure measurements. Our theoretical result of -0.13 K/GPa obviously agrees well with the experimental result. There is not a report of the pressure effect on T_c for HfN yet. The predicted dT_c/dP of -0.24 K/GPa for HfN is expected for further experimental examination.

We would like to emphasize that the opposite sign of dT_c/dP observed in these nitrides results from the competi-

TABLE II. Calculated results for λ and dT_c/dP and relevant parameters used. Experimental values of T_c and Θ_D are taken from Ref. 36. μ^* is taken from Ref. 35. Other parameters are described in the text.

Compound	HfN	ZrN	NbN
$T_c(K)$	8.83	10.00	14.94
$\Theta_D(K)$	421	515	363
μ^*	0.11	0.11	0.13
λ	0.643	0.627	0.906
$d \ln(\omega^2)^{1/2}/dP(\text{GPa}^{-1})$	8.80×10^{-3}	6.07×10^{-3}	2.93×10^{-3}
$d \ln N(E_F)/dP(\text{GPa}^{-1})$		-3.60×10^{-3}	-4.49×10^{-3}
$B_0(\text{GPa})$	344	270	350
γ_G	3.03	1.64	1.02
γ_N	1.23	0.97	1.57
φ	4.15	1.64	-0.24
ξ	-0.45	-0.27	-0.30
$dT_c^{\text{theo}}/dP(\text{K/GPa})$	-0.24	-0.13	0.05
$dT_c^{\text{exp}}/dP(\text{K/GPa})$		-0.17	0.04

tion between the electronic and phonon part of λ . We found that the contribution to dT_c/dP is mainly determined by the sum of the first two terms on the right of Eq. (2). If the contribution from the electronic part of λ outweighs the change in $\langle\omega^2\rangle$, we would have a negative φ and a positive dT_c/dP , accordingly. Therefore, the pressure derivative of T_c for NbN mainly originates from pressure-induced changes in the electronic part of the electron-phonon coupling parameter. In contrast, the pressure-induced phonon frequency shifts dominate the pressure effect on T_c in HfN and ZrN.

The expressions for γ_G , φ , and ξ can be integrated to give $\Theta_D(V) = \Theta_D(0)[V/V_0]^{-\gamma_G}$, $\lambda(V) = \lambda(0)[V/V_0]^\varphi$, and $\mu^*(V) = \mu^*(0)[V/V_0]^\xi$, respectively. Here V and V_0 are the unit cell volumes under the applied pressure and at ambient pressure, respectively. These two volumes can be related according to the first-order Murnaghan equation of state $V(P) = V(0)(1 + B'_0 P/B_0)^{-1/B'_0}$, where B'_0 is the pressure derivative of the bulk modulus. Thus, one has the pressure dependence of Θ_D , λ , and μ^*

$$\begin{aligned} \Theta_D(P) &= \Theta_D(0) \left[1 + \frac{B'_0 P}{B_0} \right]^{\gamma_G/B'_0}, \\ \lambda(P) &= \lambda(0) \left[1 + \frac{B'_0 P}{B_0} \right]^{-\varphi/B'_0}, \\ \mu^*(P) &= \mu^*(0) \left[1 + \frac{B'_0 P}{B_0} \right]^{-\xi/B'_0}. \end{aligned} \quad (8)$$

The pressure dependence of T_c is then readily obtained if one substitutes Eq. (8) into Eq. (1).

As shown by Eq. (8), we need the value of B'_0 in order to investigate the high pressure behavior of T_c . Generally, it is reasonable to take $B'_0 = 4$ for metals with the NaCl-type structure.³⁷ The theoretical results for the variation of the

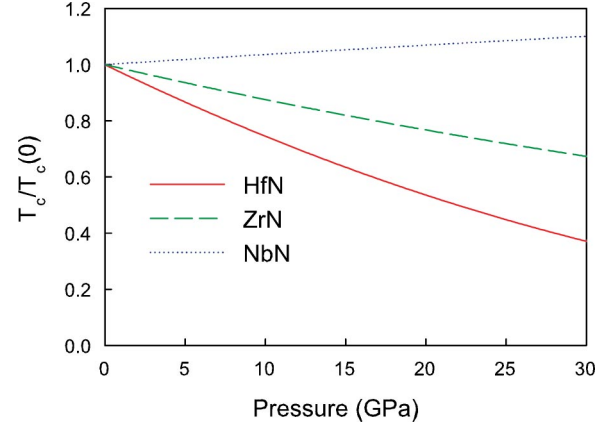


FIG. 6. (Color online) Pressure dependence of the normalized superconducting transition temperature up to 30 GPa in the transition-metal nitrides HfN, ZrN, and NbN.

normalized T_c as a function of pressure up to 30 GPa for these transition-metal nitrides are shown in Fig. 6. We found that T_c decreases with pressure and remains 3.3 K in HfN and 6.7 K in ZrN at even 30 GPa, while an increase of T_c on compression is observed for NbN. Direct high pressure measurements of T_c are required to examine our prediction.

V. CONCLUSIONS

High-pressure Raman-scattering spectra of transition-metal nitrides HfN, ZrN, and NbN exhibit two pronounced bands, which are related to the acoustic part around 200 cm^{-1} and the optical part around 550 cm^{-1} of the phonon spectrum. Transverse and longitudinal acoustic bands for Hf and Zr are well resolved, while the two bands in Nb are broad and overlapped. These characteristics are supported by the phonon density of states determined from the inelastic neutron scattering. Application of pressure shifts the peak frequency to higher values. Due to the good agreement between the Raman spectra and the phonon densities, this shift indicates pressure-induced phonon hardening.

Based on the phonon frequency shifts with pressure as well as the related parameters determined theoretically, we calculated the pressure derivative of T_c and the variation of T_c with pressure for these nitrides using the McMillan formula. The calculated values of dT_c/dP for ZrN and NbN are in excellent agreement with experiments. We have demonstrated that pressure-induced phonon frequency shifts and changes in the electronic part of the electron-phonon coupling parameter are mainly responsible for the opposite pressure derivatives of T_c observed. Extended measurements of the pressure dependence of T_c in transition-metal nitrides are in progress.

ACKNOWLEDGMENTS

We thank Z. G. Wu and R. E. Cohen for help with the calculations of elastic constants, and M. Somayazulu, L. Ehm, and P. Dera for analyzing x-ray diffraction data. This work was supported by the U.S. Department of Energy under Grant Nos. DEFG02-02ER4595 and DEFC03-03NA00144.

- *Also at: Winston Churchill High School, Potomac, MD 20854, USA.
- ¹S. V. Vonsovsky, Yu. A. Izyumov, and E. Z. Kurmaev, *Superconductivity of Transition Metals* (Springer-Verlag, Berlin, 1982), p. 180.
- ²V. V. Struzhkin, R. J. Hemley, H. K. Mao, and Y. A. Timofeev, *Nature* (London) **390**, 382 (1997).
- ³M. I. Eremets, V. V. Struzhkin, H. K. Mao, and R. J. Hemley, *Science* **293**, 272 (2001).
- ⁴V. V. Struzhkin, Y. A. Timofeev, R. J. Hemley, and H. K. Mao, *Phys. Rev. Lett.* **79**, 4262 (1997).
- ⁵M. Ishizuka, M. Iketani, and S. Endo, *Phys. Rev. B* **61**, R3823 (2000).
- ⁶N. Pessal, R. E. Gold, and H. A. Johnsen, *J. Phys. Chem. Solids* **29**, 19 (1968).
- ⁷H. Neubauer, *Z. Phys.* **226**, 211 (1969).
- ⁸H. L. Luo, S. A. Wolf, W. W. Fuller, A. S. Edelstein, and C. Y. Huang, *Phys. Rev. B* **29**, 1443 (1984).
- ⁹E. Thorwarth, M. Dietrich, and C. Politis, *Solid State Commun.* **20**, 869 (1976).
- ¹⁰T. F. Smith (private communication).
- ¹¹J. C. Phillips, *J. Appl. Phys.* **43**, 3560 (1972).
- ¹²W. Weber, H. Bilz, and U. Schröder, *Phys. Rev. Lett.* **28**, 600 (1972).
- ¹³H. G. Smith and W. Gläser, *Phys. Rev. Lett.* **25**, 1611 (1970).
- ¹⁴W. Weber, P. Roedhammer, L. Pintschovius, W. Reichardt, F. Gompf, and A. N. Christensen, *Phys. Rev. Lett.* **43**, 868 (1979).
- ¹⁵A. N. Christensen, O. W. Dietrich, W. Kress, and W. D. Teuchert, *Phys. Rev. B* **19**, 5699 (1979).
- ¹⁶A. N. Christensen, W. Kress, M. Miura, and N. Lehner, *Phys. Rev. B* **28**, 977 (1983).
- ¹⁷A. N. Christensen, O. W. Dietrich, W. Kress, W. D. Teuchert, and R. Currat, *Solid State Commun.* **31**, 795 (1979).
- ¹⁸X. J. Chen, V. V. Struzhkin, Z. G. Wu, L. Ehm, M. Somayazulu, R. E. Cohen, P. Dera, S. Kung, M. K. Mao, R. J. Hemley, and A. N. Christensen (unpublished).
- ¹⁹A. F. Goncharov and V. V. Struzhkin, *J. Raman Spectrosc.* **34**, 532 (2003).
- ²⁰A. F. Goncharov, R. J. Hemley, H. K. Mao, and J. Shu, *Phys. Rev. Lett.* **80**, 101 (1998).
- ²¹W. Spengler, R. Kaiser, and H. Bilz, *Solid State Commun.* **17**, 19 (1975).
- ²²W. Spengler and R. Kaiser, *Solid State Commun.* **18**, 881 (1976).
- ²³W. Spengler, R. Kaiser, A. N. Christensen, and G. Müller-Vogt, *Phys. Rev. B* **17**, 1095 (1978).
- ²⁴F. Gompf, J. Salgado, and W. Reichardt (unpublished).
- ²⁵W. Weber, *Phys. Rev. B* **8**, 5093 (1973).
- ²⁶H. R. Zeller, *Phys. Rev. B* **5**, 1813 (1972).
- ²⁷W. L. McMillan, *Phys. Rev.* **167**, 331 (1968).
- ²⁸P. Morel and P. W. Anderson, *Phys. Rev.* **125**, 1263 (1962).
- ²⁹X. J. Chen, H. Zhang, and H.-U. Habermeier, *Phys. Rev. B* **65**, 144514 (2002).
- ³⁰V. G. Baryakhtar and V. I. Makarov, *Zh. Eksp. Teor. Fiz.* **49**, 1934 (1965) [*Sov. Phys. JETP* **22**, 1320 (1966)].
- ³¹G. L. W. Hart and B. M. Klein, *Phys. Rev. B* **61**, 3151 (2000).
- ³²B. Palanivel, G. Kalpana, and M. Rajagopalan, *J. Alloys Compd.* **202**, 51 (1993).
- ³³B. Palanivel, G. Kalpana, and M. Rajagopalan, *Phys. Status Solidi B* **176**, 195 (1993).
- ³⁴J. W. Garland and K. H. Bennemann, in *Superconductivity in d- and f-band Metals*, edited by D. H. Douglass (American Institute of Physics, New York, 1972), p. 225.
- ³⁵U. Haufe, G. Kerker, and K. H. Bennemann, *Solid State Commun.* **17**, 321 (1975).
- ³⁶J. K. Hulm, M. S. Walker, and N. Pessal, *Physica* (Amsterdam) **55**, 60 (1971).
- ³⁷P. W. Bridgman, *Proc. Am. Acad. Arts Sci.* **76**, 1 (1945).